Effects of Controllable Transverse Magnetic Fields During the VAR Melt Process

Joshua Motley[1], John Henjum[2], Matt Cibula[1], Daniel McCulley[1], Nathan Pettinger[1], Gordon Alanko[2], and Paul King[1]

[1]Ampere Scientific, 1546 SW Industrial Way, Albany, OR 97322 USA
[2]ATI Specialty Alloys and Components, 1600 Old Salem Rd NE, Albany, OR 97321-0460 USA

Keywords: Vacuum arc remelting, VAR, control, magnetic fields, solidification, electric arc, defects

Abstract

This work describes the utilization of applied transverse magnetic fields to influence the arc dynamics during laboratory and industrial VAR melting. The arc motion was monitored with *VARmetric*™ as an external sensing platform to inform the system on the resultant direction and magnitude of the arcs due to the applied transverse magnetic field. Electromagnetic coils were mounted outside of the VAR in order to produce the near-uniform transverse magnetic field inside the furnace. These fields interact with the arc in a precise and measurable way, providing a control mechanism for arc motions and distributions. Results are provided for conditions where the applied fields were chosen such that the resultant force forces the arcs into non-ideal distributions, replicating potential deleterious operating conditions that could lead to defects. Results at both laboratory and industrial scale are provided and, wherever possible, ingots were sectioned, and the resulting grain structures were analyzed for defects.

Introduction

It is well established that arc conditions, including constricted arcs, glows, side arcs, etc., impact metal quality. Zanner *et al* not only showed that arc distributions play a critical role in ingot quality, but that "the arc has the largest, controllable, influence on the solidification involved with defect nucleation. [1]" They go on to explain that thermal transients imposed by the arc behavior play a dominant role in the creation of defects, including conditions that lead to tree rings (banding), freckles, and white spots. This prescient comment, left with little elaboration on how arcs are a controllable aspect of VAR processing, provides the basis for nearly a decade worth of effort in the development of a feedback and control mechanism that can influence the arc distributions and arc dynamics during VAR processing. This paper provides a chronological overview of one such developmental pathway, including recent trials at the industrial scale.

Recall that tree rings are caused when the mushy zone front undergoes a transient disruption; that is, when the solidus and liquidus momentarily diverge from one another. Such a transient is caused by fluctuations in the heat, mass, and momentum transfer in the region [2] [3]. Fluctuations of this type can be caused by changes in magnetic stirring conditions or in the changing arcing states such as a transition from diffuse to constricted. Freckles, on the other hand, are created during a melt-back event caused by constricted arcs which can concentrate the current in a location for an extended period. The effect of the melt-back event is to increase the flow of the lower melting temperature elements relative to the higher melting temperature elements, as captured by the Rayleigh number [4] [5] [6]. In this case, the Rayleigh number is used as a localized measure of the probability of segregation, thereby leading to the formation of freckles.

White spots, specifically discrete white spots, are thought to be formed when solute lean material freezes on the edge of the crucible-ingot interface. As the deposit grows, due to the continued deposition of material, it may grow large enough that if "knocked" off the shelf, it will tumble along the solidus line, not remelting, leaving a neutral density inclusion within the ingot [7] [8]. Constricted arcs in motion about the electrode can provide the mechanism to liberate the deposits from the crucible wall.

In the aforementioned cases, arc conditions, or changes in arc conditions, lead to the formation of the respective defects. Thus, the question presents itself: how can the arc conditions leading to these

occurrences be measured? There have been several attempts to do this, including optically [9] and thermally [10]. Of importance here, Ward [11] and Nair [12] provided a partial answer to this through the application of magnetic field sensors affixed to the VAR to investigate current flows within the VAR. Building upon this work, a passive means of investigating the arc distribution within the VAR through the external magnetic fields generated by the current associated with the distribution of arcs was investigated by Woodside [13]. In this work, Woodside further developed the concept to include considerations for additional magnetic field sources not associated with the VAR that allowed for the evaluation of the inverse problem. For example, given the magnetic flux measurement and knowledge of the magnetic fields within the environment, one can resolve the source of the magnetic flux of interest. This gave rise to the Arc Position Sensing (APS) system and, ultimately, to VARmetric.

VARmetric provides a means of measuring arc distributions in real time during operations. These measurements are currently being used to identify deleterious operating conditions and correlating those conditions with the probability of defects. For example, in Zanner's work, they referenced the fact that the application of a stirring coil for 5 minutes during VAR melting of 718 fundamentally changed the solidification structure, depositing freckles and refining the grain structure within the solidus region during which the stirring coil was actuated [1]. Computational VAR modeling showed that an interruption in the diffuse arc condition for as little as 10 minutes provides sufficient conditions for defect formation [14]. The conditions chosen for these computational studies were based on industrial observations made by VARmetric. The result from this effort, showed that the transition from a diffuse arc to a centered, focused arc and back to a diffuse arc distribution, leads to a change in the Rayleigh number and solidification velocity. The solidification velocity is seen to initially decrease in response to the change due to melt-back of the pool. Meanwhile, the Rayleigh number initially decreases and then accelerates as the system attempts to reestablish its previous equilibrium.

With this motivation, and with the fact that a functional measurement system for arc position during VAR now exists, this mechanism can be utilized as an observation platform and/or feedback for an approach to control the arc distributions. The desire to control arc distributions throughout the melt is two-fold: to 1) for identification of which type of arc distributions cause non-ideal solidification conditions by forcing known deleterious arc conditions with the control mechanism; and 2) to use the feedback provided by VARmetric measurements and a new control mechanism to prevent the conditions identified.

Arc Control and ARControl

Initial studies regarding arc control, for this effort, began in 2016 under a grant provided by the National Science Foundation. Under this grant, Cibula *et al* developed a small-scale research VAR for controls studies (Figure 1) [15]. This research VAR could strike and sustain an arc for up to 90 seconds, included a 500A, 80 V power supply, manual stinger actuator, vacuum pump, orthogonal camera viewports in the plane of the arcs, and inert gas backfill capabilities. Applying VARmetric as a measurement technique and integrating orthogonal video cameras to the sides of the chamber, they were able to simultaneously measure the arc centroid position and use image analysis to verify the position calculation. Image analysis of the orthogonal views used the luminosity of the plasma emission from cathode spots as a measure of

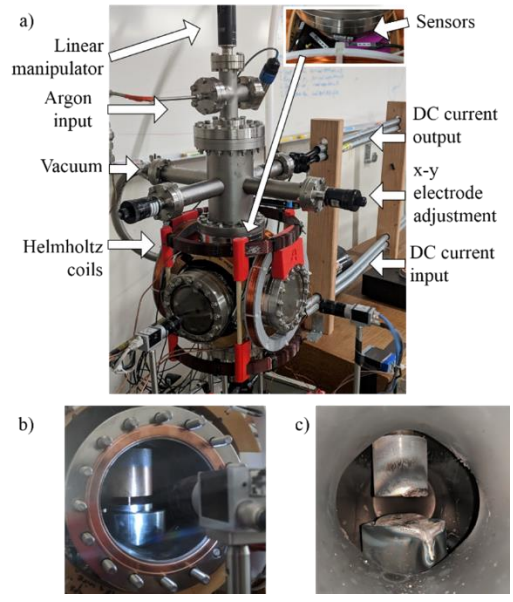

Figure 1. Experimental VAR utilized for proof of concept for the application of transverse magnetic fields as a control mechanism. – Courtesy Cibula

the arc distribution, while VARmetric APS was employed to calculate arc distributions from the magnetic fields. The two approaches resulted in a 95% confidence level between the two methodologies [16].

Once this verification effort was complete, electromagnets, in a Helmholtz coil configuration which produces a near-uniform magnetic field, were activated with feedforward control to drive arc positions from a given state to the next. Figure 2 (courtesy of Cibula *et al*) shows a heat map as the arc moved from the center of the electrode to the side through the application of the Helmholtz coils. Here, the coils were positioned so that the resulting Lorentz force acting upon the arcs was in the -y direction as depicted. Again, video image analysis was used in the orthogonal directions to verify the resultant from the applied force. This effort served as a proof of concept, and the methodology was extended to drive a controlled constricted arc into a circular motion with the centroid of the circling arc at approximately the two-thirds radius point of the electrode.

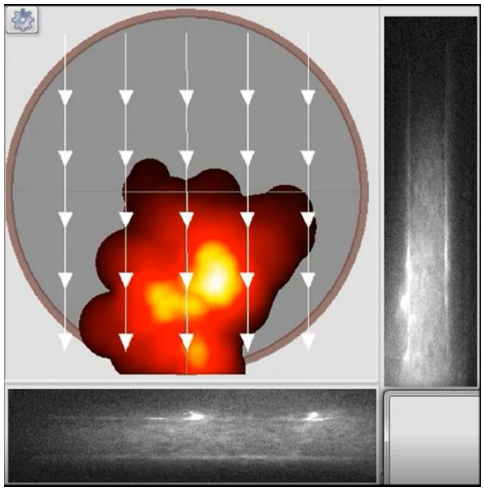

Figure 2. Application of the Lorentz force vector as a control source for arc positions and the arc positioning data. Video imagery (bottom and right) providing verification of the calculated arc location with the application of a control coil.

A shortfall of this work was that the small-scale VAR was not capable of operating in a way that maintained a liquid melt pool. In fact, operation of this VAR was limited to approximately 90-second intervals where almost no melting was allowed. In order to overcome this limitation, the research VAR unit was upgraded to include a larger vacuum chamber, more power (2500A at 60 V), larger electrodes (up to five inches in diameter) and a crucible six inches in diameter. This upgraded unit, although not a true coaxial crucible/furnace configuration, provided enough material to sustain melting for up to 15 minutes (Figure 3), producing final ingots of 3-4 inches tall. The manual stinger actuator was replaced with a digitally-controlled, linear manipulator, while the cameras were repositioned to provide a top down view to the annulus between the electrode and the crucible. The system was then outfitted with a high sensor density VARmetric unit and an orthogonal configuration of electromagnets along the funace x-y plane in a near-Helmholtz configuration. Operationally, the system was validated in a similar fashion as the original testbed; video images were used to categorize events while time synchornized mangetic field measurements were used to verify those events.

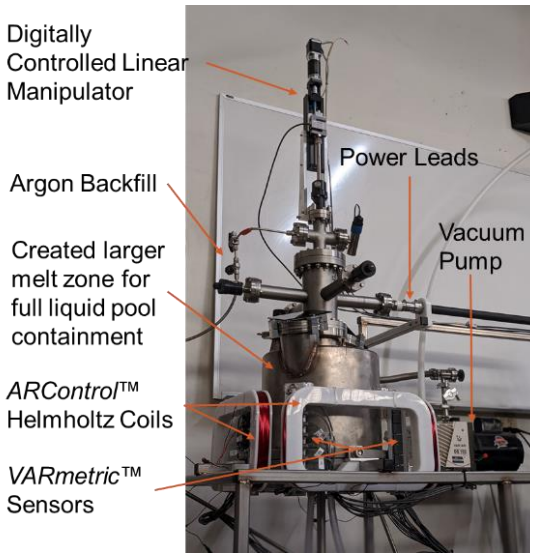

Figure 3. Updated research VAR capable of sustaining melting for up to 15 minutes with a 6-inch diameter crucible.

VARmetric APS was initially industrially validated on reactive metal furnaces with a relatively long arc gap where drip shorts are less common. One major question was: how does APS work in the presence of a short arc gap with drip shorts constantly occuring? In 2021 funding provided through the Department of Energy SBIR program allowed for the development and validation of VARmetric measurements in the presence of drip shorts. These algorithims have since been commercially implemented on VARmetric systems deployed on short arc gap furnaces. The lab experiments were conducted using the upgraded

furnace shown in Figure 3 using stainless steel as the electrodes. The ARcontrol coils provided a means of knowing the general arc locations through the known applied transverse magnetic fields and visually through video cameras, while drip shorts were occuring. This allowed for setting the arc in a known state while validating APS algorithms with drip shorts incorporated.

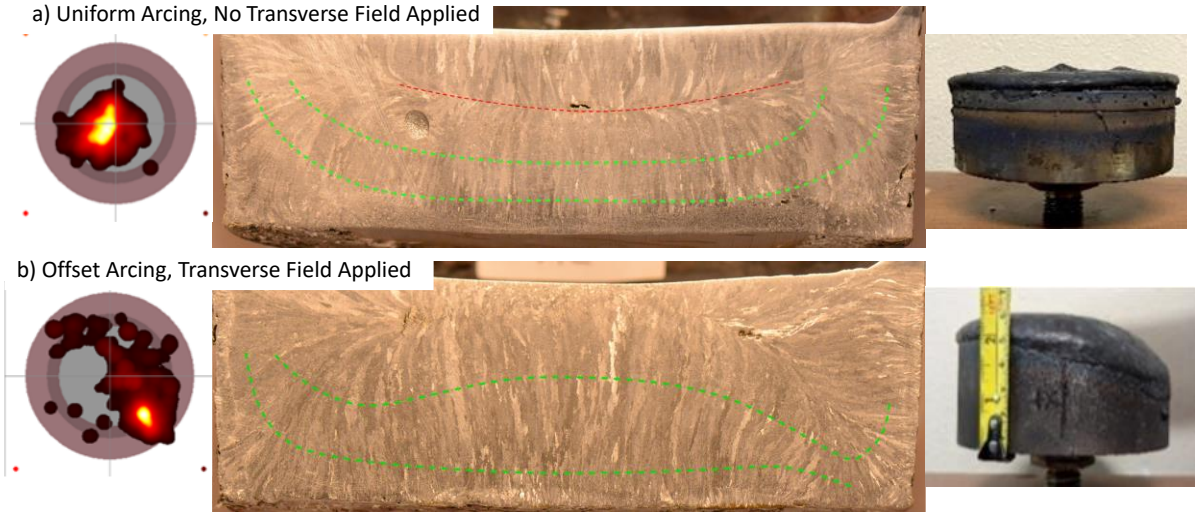

Figure 4. Effect of arc distributions on solidification in a stainless-steel ingot. a) uniform arc distributions result in a uniform solidification profile and a flat electrode tip. b) an offset arc condition induced from the applied magnetic field resulted in asymmetric solidification and electrode tip geometries. The left side shows the arc positioning distribution map during the normal melting and during the control coil field application.

From these efforts, it was established that two sets of orthoganol electromagnetic coils are sufficient to apply fields in any x-y direction to steer the arc distribution in any manner desired while the arc is localized beneath the electrode, regardless of the presence of drip shorts. Controlled experiments were run to identify the effect that a constricted arc at a location might have on the solidification of the ingot. McCulley reported results of performing these experiments on a stainless steel alloy, comparing the un-controlled, diffuse arc state with a controlled, constricted arc state [17]. Figure 4 a) provides an image of the solidification profile when a uniform arc condition is maintained throughout melting, while Figure 4 b) provides the solidification profile when the arc control shifts the arc distribution to the side of the electrode for approximately three minutes. A comparison of the final electrodes demonstrates the effect of having a constricted arc maintained within a domain. For the uniform arc condition, the electrode tip was flat, while the melt in which the transverse fields were applied melted the electrode in an asymmetric manner. The grain structures showed long columns that typically curved and pointed inward from the edges of the crucible. Consistent with industrials VARs, columnar crystals solidify along the temperature gradient, which cause them to point radially inward from the crucible, and thus provide a way to trace the solidification profile. Clearly, and not unexpectedly, the shift in solidification is a result of excess heat at the liquid boundary provided by the shifted arc distribution.

Building upon the success of these experiments, an industrial scale control unit was deployed to ATI Specialty Alloys & Components. The experiments were monitored by standard process monitoring equipment, including cameras mounted above the furnace, and with VARmetric. Figure 5 provides images of a) the VARmetric (orange strips) and the b) ARControl unit (located mid-span in the image b) installed at ATI. Here, the VARmetric was installed as a static array of sensors while the ARControl electromagnets, designed to produce a near uniform field within the melt pool region, were affixed to a linear actuator

mechanism and programmed to automatically track with the arc gap. That is, the ARControl unit moves in the vertical direction centered on the arc gap, where the location of the arc gap is measured by the VARmetric unit.

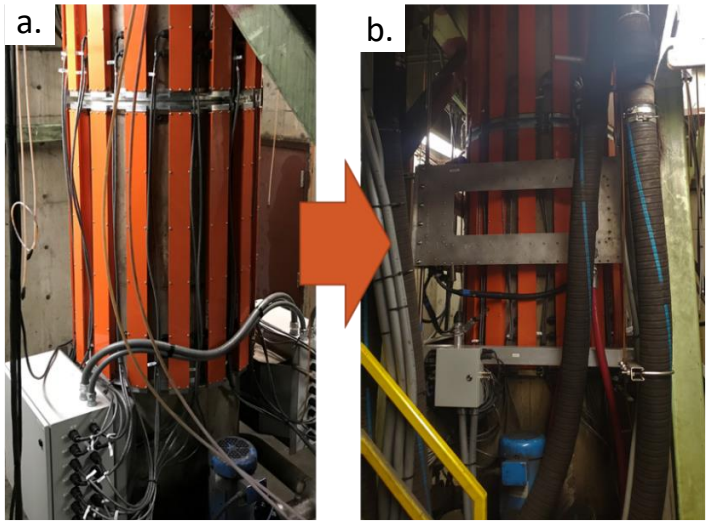

Figure 5. a) VARmetric (orange columns) and b) ARControl outfitted to a 32-inch industrial VAR melting reactive alloys for industrial experimentation.

Each coil pair is powered using a 500 amp power supply, providing enough power to the coil pairs to induce magnetic fields as strong as 33 gauss within the VAR. Prior to experiments, the magnetic field strengths applied by the coils were measured using a gaussmeter probe suspended in the radial center of the crucible. The relationship between current provided to the coils and magnetic field appeared linear, shown to be one Gauss per 15 amps. Considering that the coils produce magnetic fields outside of the furnace, the magnetic field measured by each VARmetric sensor in response to the electromagnet was measured and characterized with a linear model to provide a calibration for the electromagnet, based on the principle of magnetic superposition. This calibration was completed by actuating the electromagnetic coils vertically while applying various powers to the coils.

All of the sources of electric current near the furnace produce magnetic fields, as such, each Hall sensor measures the sum total of all these independently produced magnetic fields based on the principle of superposition. The magnetic field produced by each current source is assumed to scale linearly with the current. In light of this, correction factors are applied to each of the magnetic fields prior to calculating the location of the arc via APS. Figure 6 shows the results of this calibration. When the electromagnets are static or slowly varying, the calibrated magnetic field has a strength of 0 Tesla; however, when the electromagnet changes rapidly the magnetostatic approximation breaks down, and this method of calibration is ineffective. This behavior is expected, and, in principle, nether the stirring coil or ARControl are used during conditions where the dynamic behavior of the fields become problematic.

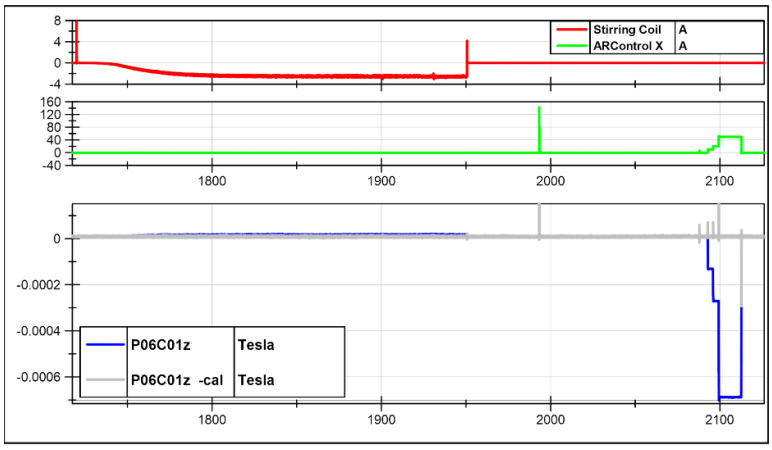

Figure 6. Measurements of Hall sensor located at Plane 6, Column 1 in the sensor array, before (blue) and after (gray) removing the influence of externally applied magnetic fields produced by the stirring coil current (red) and ARControl current (blue).

The first industrial trial was performed to ensure that the system could operate safely, considering the operations took place during reactive metal remelting, while also demonstrating the feasability at large scales. The intial experiment also showed that ARControl provided enough force to move the

arcs in the expected manner and direction. In so doing, two important considerations regarding the electrode design were:

a. The electrode surface was solid and symmetrical during the experiment.
b. The electrode allowed for adequate visibility of the melt using overhead cameras.

A "camshaft-like" electrode was constructed for the trial from billet sections of Zr4 (ATI Zircaloy-4) and Zr702 (ATI Zircadyne® 702) as shown in Figure 7. Two reference pins were added to designate the experiment window, which began on the bottom-most Zr702 billet. The constructed electrode was melted into a 20-inch diameter, water-cooled copper crucible.

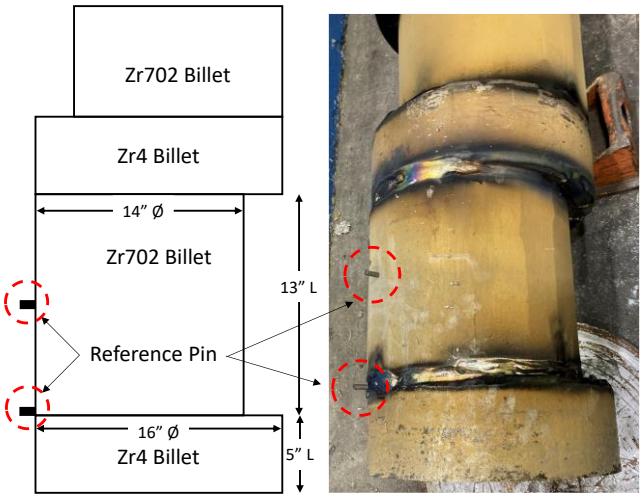

Figure 7. Electrode construction including locating pin locations.

Throughout the entirety of the melt, an axial magnetic field of 5 gauss was applied via the stirring coil. During startup, typical production practice was followed (not shown). Once a molten pool was developed and the first reference pin was melted, the furnace power was set to an experimental amperage of 6,000 amps. This furnace amperage level was maintained throughout the entirety of the experiment, which was terminated once the second reference pin was melted. After the experiment, the furnace operating parameters were returned to the normal melting practice. It should be noted that the current for the duration of the experiment is not typical for melting this alloy. 6,000 amps was percausiously chosen to safely evaluate the use of the transverse magnetic field coils during the melting of a reactive metal. Although there were 2 sets of coils for generating fields in the North/South, East/West, or any combination of the two, only the coil pair generating a field in the East/West direction was used for this trial. The following steps were taken to carry out the experiment:

1. Coils set to +25 Amps for five seconds
2. Coils turned off for 10 seconds
3. Coils set to -25 Amps for five seconds
4. Coils turned off for 10 seconds
5. Repeat steps 1-4 at: 50A, 100A, 150A, 175A, 200A, 225A, 250A, 275A, 300A, 325A, 350A, 375A, 400A, 425A

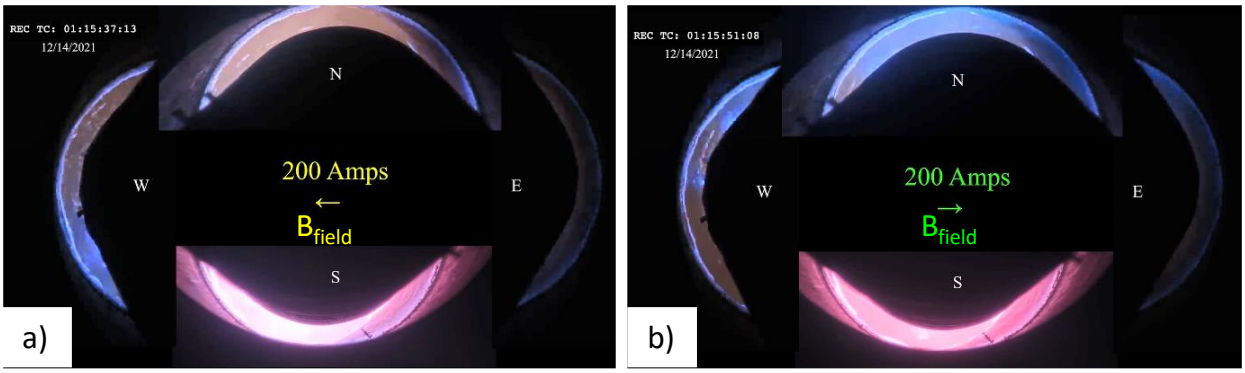

Figure 8. Overhead camera views showing a) 200A (generating 13.3 Gauss) running through the coils with the field pointed West, and b) 200A running through the coils with the field pointing East. Due to the filters used the southern end looks brighter but the east/west sections clearly indicate the arc distributions in the N/S directions.

An alternating coil field direction was chosen to ensure as much even melting across the electrode as possible, with a relaxation and operational evalution period inbetween each step. An arc response was first observed visually at 150A via the overhead cameras. Once this was observed, the 150A step was then repeated to validate the response. However, VARmetric data discussed later shows there was an arc response to lower applied fields. As the coil amperage increased, a predictable arc response was seen. A magnetic field applied in the West direction steered the arc towards the South end of the electrode, and a magnetic field applied in the East direction steered the arc towards the North end of the electrode, in agreement with the direction of Lorentz force as can be seen in Figure 8. The overhead cameras continued to display this behavior as the amperage through the magnetic coils increased.

The planes of sensors closest to the arc gap during the experiment were used to calculate the location of the arc via APS. The APS model for this furnace assumes a cylindrical electrode, however, in this experiment the electrode was composed of a series of offset stacked cylinders of varying size. While this difference between the model and the physical system is expected to introduce some error into the results from the ideal geometry, APS uses an additional calibration factor to correct for real-world deviations from the idealized model. This 'geometric correction' is applied as an offset to the magnetic field measurements that scales linearly with the furnace current, similar to the methodology for removing the magnetic fields produced by the electromagnets. However, in this case, the geometric correction is a measurement of the magnetic field for each sensor that is representative of the average magnetic field measured by the sensor when the arc distribution is, on average, centered in the furnace.

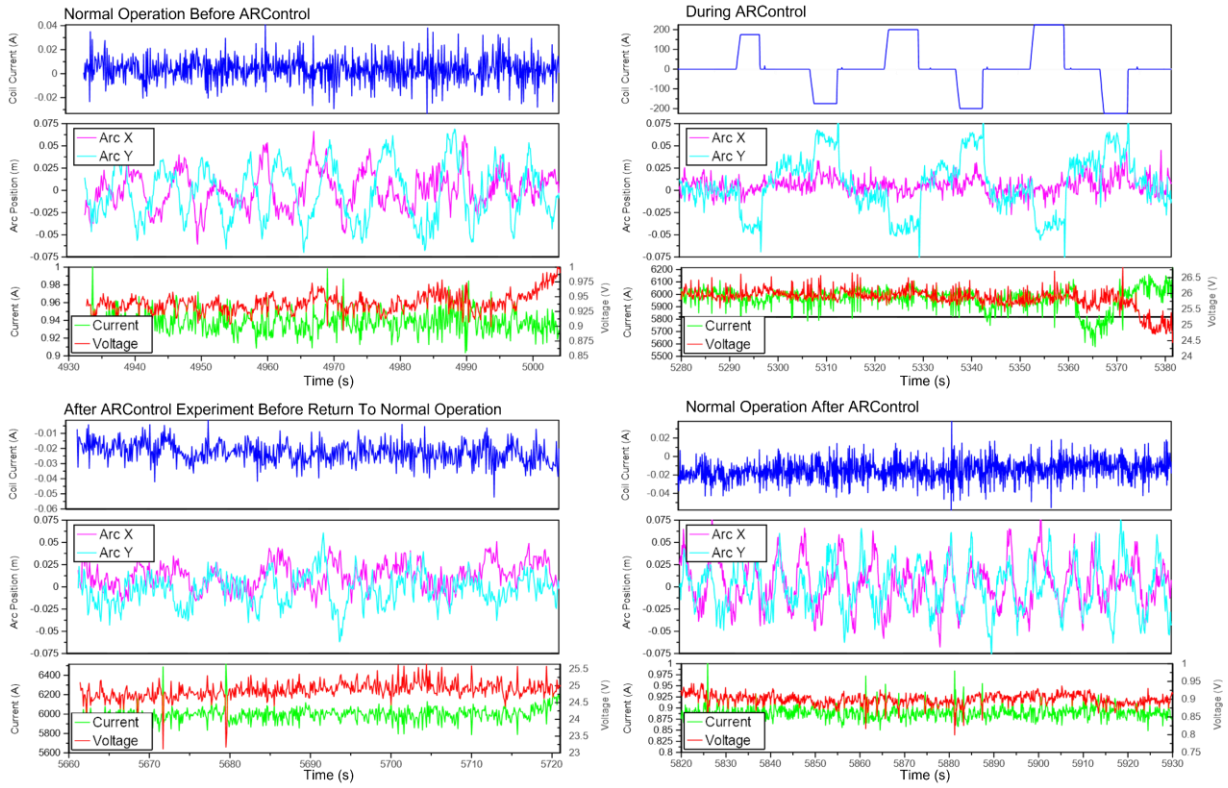

Figure 9. Measurements of the furnace current (red), furnace voltage (green), ARControl current (blue), and arc x (cyan) and y (magenta) position; during normal operation before the experiment (top left), during the experiment at a reduced current (top right), right after the experiment (bottom left), and after returning to normal operating conditions (bottom right). The stirring coil current was on and static in one direction during the test. Current and voltage are shown as a percentage before/after the experiment to protect proprietary nature of the melt parameters. The crucible diameter was 50.8 cm.

The APS results before, during, and after the experiment are presented in Figure 9 where the actual voltage and current measurements have been normalized. Before and after the experiment, the arc centroid slowly rotated around the furnace with an amplitude of about 6-7 cm and period of 8 s. After increasing the arc gap, stopping the stirring coil switching, and setting the current to 6 kA the magnitude of the arc rotations reduced to 4-5 cm. The top right plots in Figure 9 shows the direct response in APS due to the applied field pulses. Application of the ARControl x-fields shifted the arcs along the y-axis during the experiment and reduced the oscilation magnitude in the x direction. As the experiment progressed, the y and x position measured began to oscillate more, presumably due to changes in the geometry of the electrode tip as the melt continued. It is noteworthy to mention that the ARcontrol coils did not noticably affect the furnace operating current or voltage. Figure 10 a) shows the arc off set as a function of applied coil current, while b) shows how the fields applied affected the arc motion over the course of the experiment. Increasing the current through the electromagnet increased the offset to the arc position from 25 A to 100 A, but up to 400 A the APS-measured arc offset was limited to 6-9 cm in the +y direction and 5-6 cm in the -y direction. This behaviour was not symetric between the y and -y axis, this may be due to deviations in the corrections previously discussed or from the electrode geometry evoluation due to arc melting.

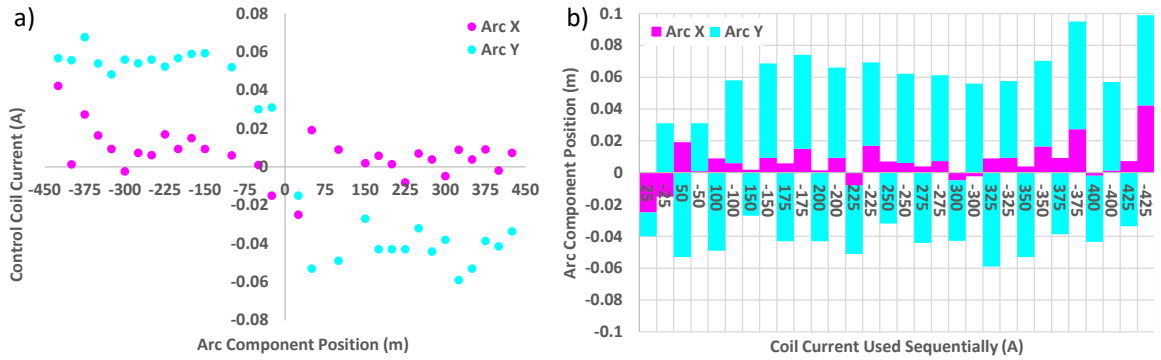

Figure 10. a) Arc x and y position as a function of coil current and direction. b) the arc x and y position shown in sequential order of coil power application.

The electrode section during the experiment had a diameter of 14 inches (35.6 cm) or radius or 17.8 cm. APS never showed arcs extending out to the edge of the electrode, in fact the max radial distance of the oscillating arc during normal operation was around 7.5 cm. The nature of the APS measurement indicates the centroid or averaged center of a distribution of arcs, with the edge of the electrode being the limit of the arcs (excluding side arcing). This may indicate the assumed circular gaussian arc distributions have a radius of approximately 10.3 cm during a normal operation, covering 33% of the electrode surface at any given time as demonstrated in Figure 11. However, much more investigation needs to be done to elucidate this relationship. Considering that the video images continued to brighten during the test, it is believed that this behavior is a result of the fact that the centroid of the arc distribution is, in fact, limited and is forced to deviate from a Gaussian distribution as the arc is forced to one side of the electrode. That is, the distribution of the arc likely changes from an axisymmetric distribution about the arc centroid to an oblong or asymmetric distribution as it is pushed against the electrode boundary. Under these conditions the arc centroid would remain static while the distribution of the arc would deform.

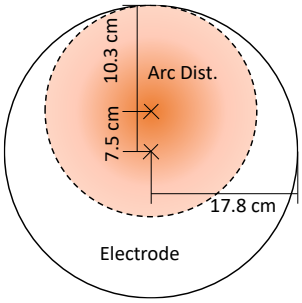

Figure 11. Assumed ideal arc distribution with a limit at the edge of the electrode.

Additional testing of the ARControl unit is underway with the application of any combination of x-y transverse fields and is expected to provide additional information regarding the relationship between ingot

quality and arc disbributions. As this study is in the early stages, additional plans are for longer arc control runs, ingot sectioning and analysis leading to a better understanding of the direct relationship between the two. Additionally, computational fluid dynamics modeling is being performed, based upon the heat flux measurement, to predict the probability of defects.

Discussion

As demonstrated over several scales, the application of transverse magnetic fields can be utilized in the control of vacuum arc furnace melting. Conceptually speaking, the application of such control provides tremendous latitude around product quality optimization. Used sparingly, it could be employed to correct transient operating conditions such as constricted arcs or glows in order to avoid the creation of defects. Used dynamically, it could be utilized as a full feedback mechanism for tailoring/optimzing the heat flux throughout the VAR process. Recognizing that despite the best efforts to ensure repeatability in VAR operations, there is no gaurantee of such. Also recognizing that technologies are asking more and more of the materials available, dictating tighter controls over the metal quality, new methods are required to ensure successful development of those metals. VARmetric provides a commercially available measure of such quality. VARmetric plus ARControl may be able to achieve finer control over heat flux variations, thus providing a deterministic means of ensuring metal quality.

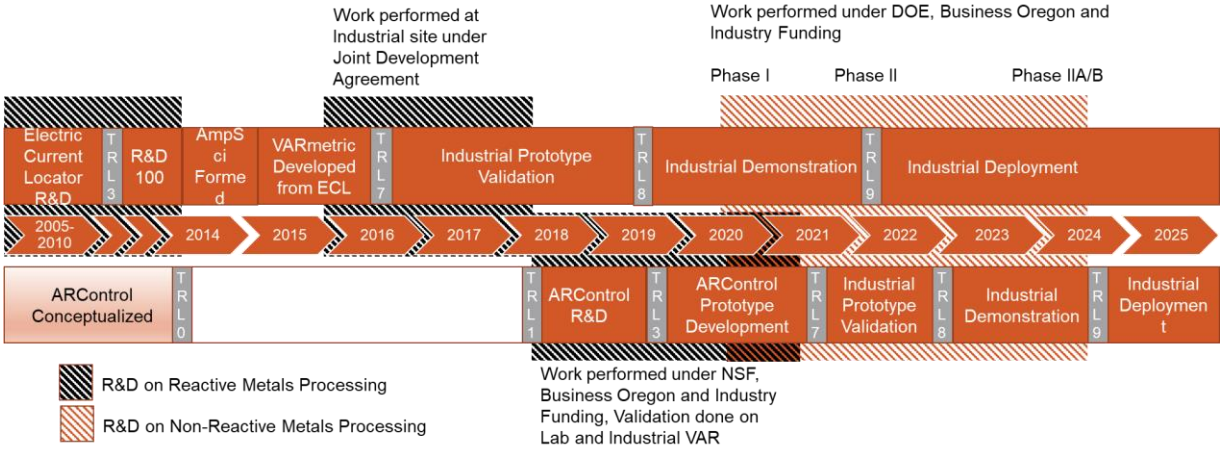

Figure 12. VARmetric and ARControl developmental timelines.

The overall development pathway for VARmetric and ARControl are provided in Figure 12. The Electric Current Locator and Arc Position Sensing was conceived and developed from 2005 to 2010 at the National Energy Technology Lab based upon funding and guidance of the Specialty Metals Processing Consortium. In 2014, industrial hardening of the technology became a primary focus, and between 2015 and 2020, these efforts included hardware and software development leading to the VARmetric technology deployed today. In parallel, the ARControl technology development began in 2017 based upon funding from the National Science Foundation. Over the course of the past 5 years, the technology has been developed from laboratory testing to industrial realization with several units residing in the field. To date, these systems are being used in scoping studies as presented here. It is expected that over the course of the next one to two years, additional validation on the efficacy of ARControl as a VAR control mechanism will ensue.

Acknowledgements

This work was partially supported by NSF SBIR Grants 1647655 and 1831255 and the Department of Energy SBIR Grant DE-SC0020980. The authors would also like to recognize ATI Specialty Alloys and Components for their participation and support for this work.

References

[1] W. R. E. R. Zanner F, "On The Origin of Defects," *Proceedings of the 2005 International Symposium on Liquid Metal Processing and Casting,* pp. 13-27, 2005.

[2] R. W. M. J. P. L. a. M. M. X. Xu, "Tree Ring Formation during VAR of Alloy 718: Part 1. Experimental Investigation," *Met. Trans. A,* vol. 33, pp. 1795-1803, 2002.

[3] W. Z. a. P. L. X. Xu, "Tree Ring Formation during VAR of Alloy 718: Part 2. Mathematical Modeling," *Met. Trans. A,* vol. 33A, pp. 1805-1815, 2002.

[4] J. K. P. &. L. X. Valdés, "On the Formulation of a Freckling Criterion for Ni-Based Superalloy Vacuum Arc Remelting Ingots," *Metal Mater Trans A,* vol. 44, pp. 2408-2416, 2010.

[5] T. M. P. &. W. H. Murphy, "The breakdown of single-crystal solidification in high refractory nickel-base alloys," *Metall. Mats. Trans. A,* pp. 1081-1094, 1996.

[6] P. W. T. C. S. Auburtin, "Freckle formation and freckle criterion in superalloy castings," *Metall Mater Trans B,* vol. 31, pp. 801-811, 2000.

[7] X. &. B. M. &. W. R. &. J. M. Wang, "The effect of VAR process parameters on white spot formation in INCONEL1 718," *Journal of Materials Science,* vol. 39.

[8] J. K. M. S. J. v. d. A. R. a. F. Z. B.K. Damkroger, "The influence of VAR processes and parameters on white spot formation in Alloy 718," in *International symposium on superalloys 718, 625, 706 and derivatives*, Pittsburgh, PA, 1994.

[9] R. M. a. W. R. L. Aikin, "A new optical emission monitor for vacuum arc remelting," in *Liquid Metal Processing & Casting Conference*, Santa Fe, NM, 2009.

[10] R. L. a. S. G. Williamson, "Current paths during vacuum arc remelting of alloy 718," in *Superalloys 718, 625, 706 and Various Derivatives*, 2001.

[11] R. M. a. M. H. J. Ward, "Electrical and magnetic techniques for monitoring arc behaviour during VAR of INCONEL1 718: Results from different operating conditions," *Journal of materials science,* vol. 39.24, pp. 7135-7143, 2004.

[12] B. G. a. W. R. M. Nair, "An analysis of the use of magnetic source tomography to measure the spatial distribution of electric current during vacuum arc remelting," *Measurement Science and Technology,* vol. 40, no. 4.

[13] R. Woodside, "Arc distribution and motion during vacuum arc remelting process as detected with a magnetostatic approach," Oregon State University, Corvallis, Oregon, 2010.

[14] J. K. K. K. P. C. M. a. M. A. Motley, "Measurement of the Spatio-temporal distribution of arcs during vacuum arc remelting and their implications on VAR solidification defects," in *Proceedings of the Liquid Metals Processing & Casting Conference*, Birmingham, England, 2019.

[15] M. K. P. a. M. J. Cibula, "Feedback-based control over the Spatio-temporal distribution of arcs during vacuum arc remelting via externally applied magnetic fields," in *Proceedings of the Liquid Metals Processing & Casting Conference*, Birmingham, England, 2019.

[16] M. K. P. a. M. J. Cibula, "Feedback-based control over the Spatio-temporal distribution of arcs during vacuum arc remelting via externally applied magnetic fields," *Met. Trans B,* vol. 51, no. 11, 2020.

[17] D. M. J. C. M. a. K. P. McCulley, "Elucidating the relationship between arc behavior and solidification defects during vacuum arc remelting of superalloys," *2022 151st Annual Meeting & Exhibition Supplemental Proceedings. The Minerals, Metals & Materials Series,* pp. 994-1003, 2022.